



# Effect of Concentration Variation on Optical and Structural Properties of TiO<sub>2</sub> Thin Films

Sabastine Chinedu Ezike

Department of Physics, Modibbo Adama University of Technology, Yola, Adamawa State, Nigeria

\* Corresponding author email: [chineduezike81@gmail.com](mailto:chineduezike81@gmail.com)

Received: 10 February 2020 / Accepted: 28 February 2020 / Published: 05 March 2020

## ABSTRACT

Concentrations in weight percent (5- 25 wt %) of TiO<sub>2</sub> films used to optimize the film formation. The TiO<sub>2</sub> films on glass substrates successfully obtained by spin-coating process using TiO<sub>2</sub> nanopowder as precursor. Ultraviolet-Visible (UV-Vis), Scanning Electron Microscopy (SEM) equipped with Electron Diffraction X-ray (EDX) and X-ray Diffractometer (XRD) techniques used to characterize the films. The result of electron transport material (TiO<sub>2</sub>) showed that film prepared from 15 wt % of TiO<sub>2</sub> solution and annealed at 450 °C has highest transmittance at visible light region with indirect optical band gap of 3.24 eV which corresponds to wavelength of 382 nm whereas 20 wt % has indirect band gap of 2.99 nm equivalent to 414.7 nm . The chemical analysis from Electron Diffraction Spectroscopy (EDS) of the material shows titanium and oxygen present at L and K-shells, respectively. The sample crystallized with preferred orientation at (101) from XRD analysis.

**Keywords:** TiO<sub>2</sub>, Thin Film, Electron Transport Material, Spin coating, concentration variation.

## 1 Introduction

Titanium dioxide (TiO<sub>2</sub>) used for environmental and global applications is one of the most studied materials. The oxidizing and reducing nature of photo-generated holes and electrons, respectively, in TiO<sub>2</sub> produce superoxide [1, 2]. TiO<sub>2</sub> nanoparticle films are used in photo semiconductor, photo-oxidation of water and photo-catalysis [3, 4]. Photo semiconducting titanium dioxide thin films are important in processes where the transparency of the film required. Nanoparticle structure of TiO<sub>2</sub> film provides high internal surface area to allow enough quantity of dye to absorb light very well and ensures that each dye molecule is in good contact with the photoanode and electrolyte. It also occupies the pores of the film in dye sensitized solar cells [5]. TiO<sub>2</sub> as N-type semiconducting material has wide band gap with indirect energy band gap of 3.2 eV (anatase) and 3.02 eV (rutile) [6]. Several methods employed in

preparation of TiO<sub>2</sub> films include electron-beam evaporation [7,8], sputtering [9], sol-gel and dip coating, chemical vapour deposition [10] and spin-coating process [11-13]. Among the methods used, spin-coating offers advantages of low temperature processing, low cost, ease of coating large area and suitable for porous film preparation.

The photo-semiconducting activity of TiO<sub>2</sub> could be modified by the concentration of the starting materials and this affects its physicochemical properties such as crystallinity, crystal structure, particle size, and surface area [14]. The extent of TiO<sub>2</sub> transparency may result in changes in photo-semiconducting activity due to shift in band edges [15]. TiO<sub>2</sub> films are expected to be transparent at the visible region. The concentration of the precursor affects the transparency of TiO<sub>2</sub> films [16]. Pathak *et al.* [17] reported the effect of doping TiO<sub>2</sub> photoanode with aluminium on the performance and stability enhancement and the efficiency and stability



upon UV exposure of the devices improved. Fakhruddin *et al.* [18] showed the performance and long-term stability of planar device with compact TiO<sub>2</sub> layer, mesoporous devices with bare and TiCl<sub>4</sub>-treated TiO<sub>2</sub> nanorods scaffolds showed that mesoporous device exhibited more stability than the planar device. There are three structures of TiO<sub>2</sub> crystal, which are anatase, rutile and brookite. Among the three, anatase has preferable photocatalytic properties to others [19]. The untreated TiO<sub>2</sub> thin films are amorphous in nature and transformation to anatase or rutile phase do depend on annealing temperature. The anatase phase occurs at temperature range of 400 °C to 600 °C and anatase - rutile phase exists at temperature of 800 °C while wholly rutile phase at 1000 °C [20]. Senthil *et al.* [21] reported fabricated TiO<sub>2</sub> thin films with anatase phase and grain size of 19 nm. Elfanaoui *et al.* [22] synthesized TiO<sub>2</sub> thin films with energy band gap of 3.7 eV. Zharvan *et al.* [23], fabricated TiO<sub>2</sub> thin films with anatase phase by spin coating technique and the optical band energy gap of the resulted TiO<sub>2</sub> films were in the range of 3.70 to 3.76 eV.

However, study of the solution's concentration variation on optical and structural properties has not been reported at the time of this research. In the present work, TiO<sub>2</sub> nanoparticles were deposited by spin-coating technique and films at concentrations of 5 – 25 wt % annealed at two different temperatures (450 and 500 °C). The prepared films after annealing have been employed to study the optical and structural properties.

## 2 Research Methodology

Glass substrates were cut to dimensions of 2 cm x 2 cm. The substrates were cleaned with detergent and rinsed with distilled to remove oily stains and debris. Then the substrates were put in staining jar and acetone is introduced and subjected for ultrasonic cleaning with the help of sonicator for 15 minutes at 27 °C to remove organic forts and water molecules from the substrates. The acetone-cleaned substrates were ultrasonically cleaned in ethanol at the same conditions to remove more water and acetone remnants. Lastly, they were cleaned in

Isopropanol alcohol (IPA) at the same conditions to remove remaining water on the substrates and blown dried with nitrogen gas. Commercial microscope glass substrates were cleaned in ultrasonic bath (Stuart heat-stir UC152) with detergent, distilled water, acetone, ethanol and IPA each for 15 min at 30 °C, respectively and dried with nitrogen gas [24]. Different weight percents (wt %) (5 - 25 wt %) of TiO<sub>2</sub> precursor solutions were prepared from titanium dioxide nanopowder (Aldrich) with ethanol (Analytical grade, Merck) as solvent using equation (1) [25].

Weight percent (wt %)

$$= \frac{\text{Mass of Solute (g)}}{\text{Volume of solution (ml)}} \times 100 \% \quad (1)$$

Ohaus weighing balance (Adventure pro) was used to measure respective masses of TiO<sub>2</sub> powder at different weight percent. The precursor solutions prepared from measured masses on weighing balance.

The precursor solutions were spin-coated on glass substrates at 4000 rpm for 30 seconds using spincoater (WS-650MZ-23NPP Laurell) and dried at 125 °C for 5 min. The spin-coating process of TiO<sub>2</sub> precursor solution was performed twice and Smooth and milky solutions were obtained. The glass substrates deposited TiO<sub>2</sub> precursor solution were annealed at 450 °C and 500 °C for 30 min to form compact layer. X-ray diffraction (Rigaku D-Max) with fixed Cu-Kα line (k=1.5406 Å) was used for recording X-ray diffraction spectra operating at 30 kV and 30 mA at room temperature in the 2θ range of 20-70°. Scanning electron microscope (SEM) equipped with electron diffraction x-ray was operated at 15 kV at higher magnification to study the morphology and composition of prepared samples. Ultraviolet visible (UV-VIS) spectroscopy (Lambda 35 Perkin- Elmer) was done in the range of 300 to 800 nm to study the optical properties.

## 3 Results and Discussion

### 3.1 Optical Properties

Different concentrations (5 to 25 wt %) of TiO<sub>2</sub> were prepared and treated at temperatures of 450 °C and 500 °C. Figure 1 shows graph of

transmittance against wavelength of  $\text{TiO}_2$  prepared from concentrations of 5 to 25 wt % at step- size of 5 w % with post deposition treatment at 450 °C . Transmittance values increase with increase in wavelength. In the films annealed at 450 °C, concentration increase from 5 to 15 wt % is directly proportional to the transmittance of the films.

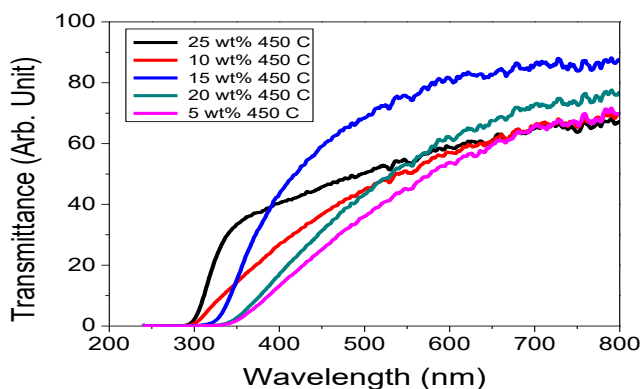


**Figure 1:** Concentration variation of  $\text{TiO}_2$  films annealed at 450 Degrees Centigrade

Further increase in concentration of the films, reduces the transmittance of the films as seen in 20 wt % and 25 wt % when annealed at 450 °C. The sample prepared from 15 wt % has the highest transmittance. Also, films annealed at 500 °C as shown in Figure 2 have increase in visible light transmission from 5 to 20 wt % and declined at 25 wt % with onset transmittance value at 298 nm.

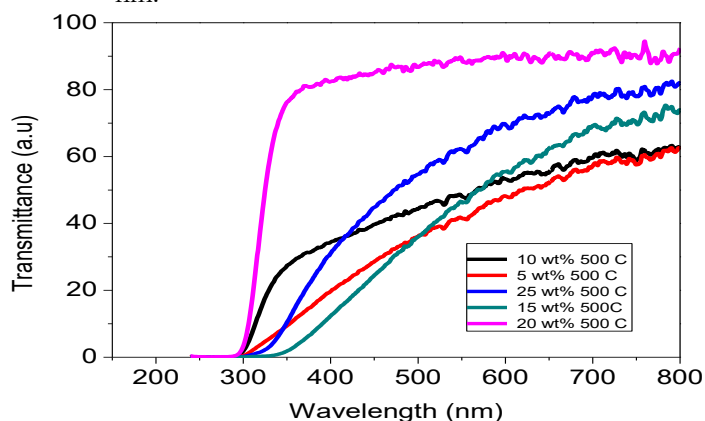


**Figure 2:** Concentration variation of  $\text{TiO}_2$  films annealed at 500 Degrees Centigrade

In comparing the concentrations of the optimized films annealed at both 450 °C and 500 °C, 20 wt % of the films annealed at 500 °C has lower transmittance than that of the films annealed at 450 °C. Considering its application in

solar cells as a buffer layer, it is required to transmit visible light to the active material and the film prepared from 15 wt % (450 °C) has higher transmittance value than 20 wt % (500 °C). The absorbance properties of the films are shown in Figure 3. This shows that  $\text{TiO}_2$  film prepared from 20 wt % annealed at 500 °C has higher absorption value than the sample prepared from 15 wt % annealed at 450 °C. The optical absorption spectra for treated samples show blue shifts due to quantum effect with increase in annealing temperature. Absorption range of  $\text{TiO}_2$  film prepared from 20 wt % is within 250 to 350 nm and 250 to 380 nm for 15 wt % prepared film annealed at 450 °C. This could likely cause by increase in crystallite size and the induced oxygen vacancies at higher annealing temperature. This could cause donor impurities to move the absorption edge to higher energies due to the presence of created defect sites [26].

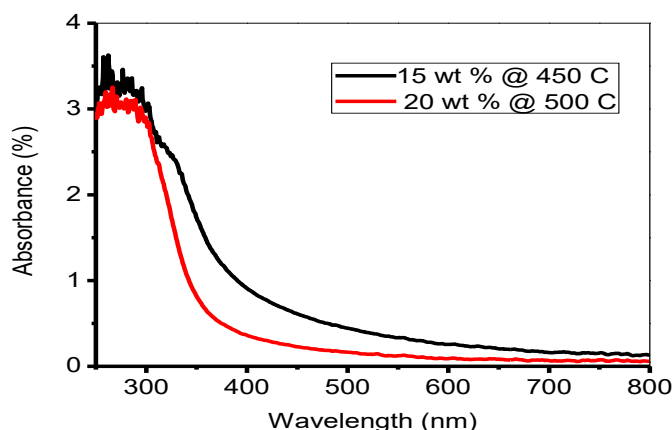


**Figure 3:** Plot of absorbance versus wavelength of 20 wt % and 15 wt % samples of  $\text{TiO}_2$  films annealed at 450 °C and 500 °C.

The optical band gap energy of  $\text{TiO}_2$  thin films was obtained by Tauc plot and shown in Figure 4. Comparing their optical energy band gaps, 20 wt % film annealed at 500 °C and 15 wt % film annealed at 450 °C they have 2.99 eV and 3.24 eV of energy band gap, respectively. The energy band gap was deduced as reported by Ezike and Okoli [27]. Increase in annealing temperature leads to decrease in band gap. The 20 wt % prepared sample annealed at 500 °C absorbs at visible region while 15 wt % sample annealed at 450 °C absorbs at ultraviolet region.

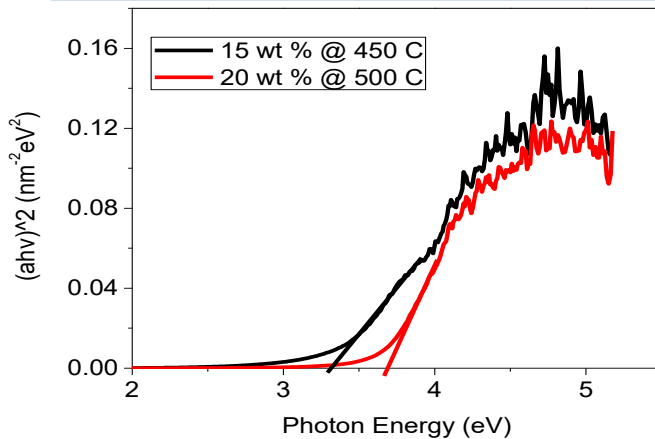


**Figure 4:** Plot to determine the energy band gap of TiO<sub>2</sub> films annealed at 450 °C and 500 °C.

This shows that 15 wt % film annealed at 450 °C when deployed in solar cells transmits visible light and blocks ultraviolet radiation. This is because, 15 wt % (450 °C) transmits about 88 % of visible unlike the film prepared from 20 wt % (500 °C) which absorbs visible light.

### 3.2 Micro-structural Properties

The SEM images of TiO<sub>2</sub> are shown in Figure 5 (a) and (b).

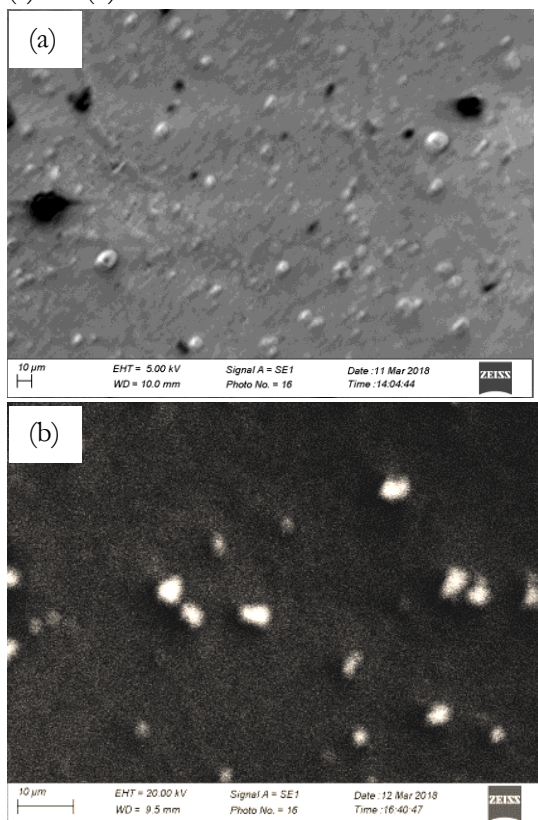


**Figure 5:** SEM image of (a) 15 wt % TiO<sub>2</sub> films annealed at 450 °C and (b) 20 wt % TiO<sub>2</sub> films annealed at 500 °C.

The images showed that the particles are spherical in shape with image in Figure 5 (a) having poor agglomeration and aggregation during particle growth process at higher calcinations temperature and concentration. The sample prepared from 20 wt % annealed at 500 °C (Figure 5 (a)) showed larger crystal size than 15 wt % annealed at 450 °C (Figure 5 (b)). This supports optical properties of the samples showing that sample prepared from 20 wt % annealed at 500 °C has higher absorbance and lower transmittance than 15 wt % prepared film at visible region.

### 3.3 Elemental Composition Analysis

The elemental composition of the material thin film deposited was characterized to ascertain the actual elements or the level of purity contained in the material. Emission of energy gives the characteristics energy level and the element contained in the material. The sharp lines are the characteristic lines of elements from which they are emitted. Figure 6 shows the electron diffraction spectroscopy of TiO<sub>2</sub> thin film. There are peaks of Titanium (Ti) and Oxygen (O) present at L and K- shells, respectively. The presence of these elements confirms that TiO<sub>2</sub> film was deposited. The weight percentages of both elements are 38.90 and 61.10 % for titanium and oxygen, respectively. This was performed at voltage of 5 kV and magnification of 824.

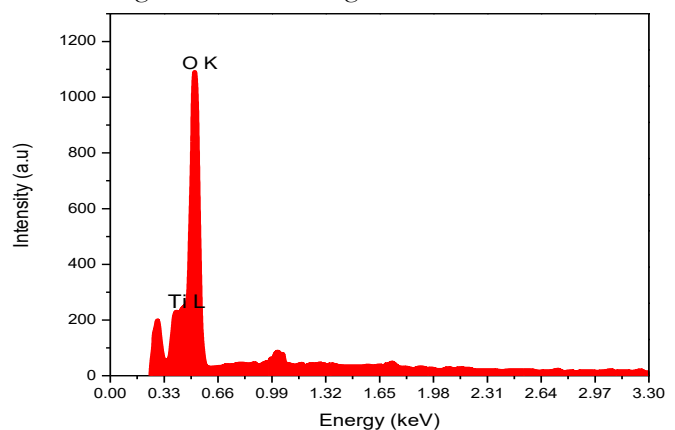


**Figure 6:** Elemental composition of TiO<sub>2</sub> thin film.

### 3.4 Structural Characterization

Figure 7 shows XRD spectra pattern two samples of TiO<sub>2</sub> prepared from 15 wt % and 20 wt % with post-deposition treatment at 450 °C and 500 °C, respectively.



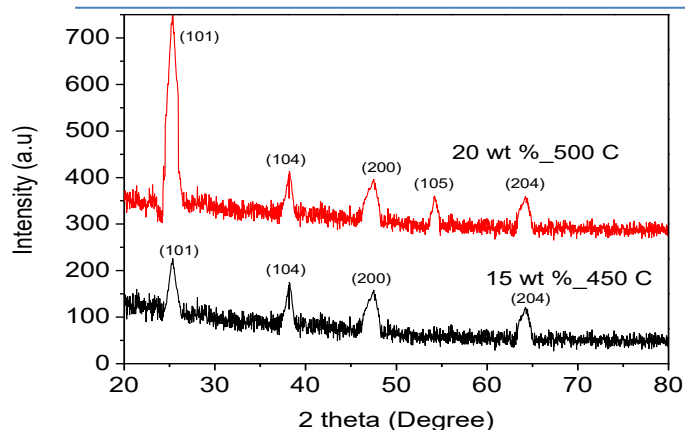


**Figure 7:** X-ray diffraction patterns of 15 wt % and 20 wt % annealed at 450 °C and 500 °C, respectively of TiO<sub>2</sub>.

In the XRD pattern, TiO<sub>2</sub> prepared at 500 °C has maximum peak with anatase phase corresponding to (101) (JCPDS file no. 861167) was observed at  $2\theta = 25.4^\circ$  [28]. The sample treated at 450 °C has maximum intensity peak corresponding to plane (101) as in sample treated at 500 °C, but the peak was observed at  $2\theta = 25.2^\circ$  of the anatase structure (JCPDS file no. 731764). The intensity of the peak (101) increased as the samples post-deposition treatment increased. The 20 wt % film annealed at 500 °C was well crystallized at plane (101) more than sample prepared from 15 wt % annealed at 450 °C. This shows that sample prepared from 20 wt % annealed at 500 °C with higher intensity peak corresponding to (101) has larger crystallite size than the 15 wt % prepared sample annealed at 450 °C. The average crystallite size was estimated using Scherer's equation, in equation (2), to the major peaks of the XRD data and taking an average [29].

$$D = k\lambda / \beta \cos\theta \quad (2)$$

where D is average crystallite size in angstroms (Å) and K is the shape factor (0.94),  $\lambda$  is the wavelength of X-ray radiation (Cu K $\alpha$  = 1.5406),  $\beta$  is the Full Width at Half Maximum (FWHM).<sup>1</sup> The average crystallite size of the prepared films at 500 °C is 12.19 nm and at 450 °C is 10.05 nm. Increase in average crystallite size could be attributed to the concentration and temperature post-deposition treatment of the samples.

## 4 Conclusions

It was observed from the result of electron transport material (TiO<sub>2</sub>) prepared from 15 wt % of TiO<sub>2</sub> nanopowder, annealed at 450 °C has best optical performance at visible light region as confirmed by morphological and structural characterizations. The optical band gap of the film is 3.7 eV, which shows material with high transmittance value. SEM image showed that 20 wt % sample has higher average crystallite size of 12.19 nm, which suggests more absorption of visible light, than 15 wt % film of 10.05 nm prepared sample. The chemical analysis by EDX of the material shows titanium and oxygen at L and K-shells, respectively. The sample crystallized with preferred orientation at (101) from XRD. This shows that 15 wt % annealed at 450 °C is preferred as a transport material in solar cell fabrication.

## 5 Declarations

### 5.1 Study Limitations

There was non-availability of atomic force microscope for roughness analysis.

### 5.2 Acknowledgements

The author would like acknowledge Rasheed Abiodun Jimoh of the Department of Materials Science and Engineering, Kwara State University, Malete and Mr. A. Elechi of the African University of Science and Technology, Abuja, for laboratory assistance.

### 5.3 Competing Interests

Author declares that there is no conflict of interest exist.

## How to Cite this Article:

S. Ezike, "Effect of Concentration Variation on Optical and Structural Properties of TiO<sub>2</sub> Thin Films", *J. Mod. Mater.*, vol. 7, no. 1, pp. 1-6, Mar. 2020. doi: 10.21467/jmm.7.1.1-6

## 6 References

- [1] X. Kang, S. Liu, Z. Dai, Y. He, X. Song, Z. Tan, "Titanium Dioxide: From Engineering to Applications," *Catalyst*, vol. 9, pp. 191, Feb. 2019.
- [2] M. H. Farooq, I. Aslam, A. Shuaib, H. S. Anam, M. Rizwan, Q. Kanwal, "Band Gap Engineering For Improved Photocatalytic Performance Of Cus/Tio2 Composites Under Solar Light Irradiation," *Bull. Chem. Soc. Ethiop*, vol. 33, no. 3, pp. 561-571, Jul. 2019.

- [3] Y. Wang, C. Sun, X. Zhao, B. Cui, Z. Zeng, A. Wang, G. Liu, H. Cui, "The Application of Nano-TiO<sub>2</sub> Photo Semiconductors in Agriculture" *Nanoscale Res Lett*, vol. 11, pp.529, 2016.
- [4] S. Higashimoto, "Titanium-Dioxide-Based Visible-Light-Sensitive Photocatalysis: Mechanistic Insight and Applications," *catalyst*, vol. 9, pp. 201, Feb. 2019.
- [5] K. Sharma, V. Sharma, S. S. Sharma, "Dye-Sensitized Solar Cells: Fundamentals and Current Status," *Nanoscale research letters*, vol. 13, no.1, pp. 381, Nov. 2018.
- [6] Y. Nam, J. H. Lim, K. C. Ko, J. Y. Lee, "Photocatalytic activity of TiO<sub>2</sub> nanoparticles: a theoretical aspect," *J. Mater. Chem. A*, vol. 7, issue 23, pp. 13833-13859, May 2019.
- [7] A. Jilani, M. S. Abdel-wahab, A. H. Hammad, "Advance Deposition Technique for Thin Film and Coating", Modern Technologies for Creating the Thin-film Systems and Coatings, N. N. Nikitenkov, *Intechopen*, Mar. 2017.
- [8] S. C. Ezike, G. M. Z. Kana, A. O. Aina, "Progress and Prospect on Stability of Perovskite Photovoltaics," *J. Mod. Mater.*, vol. 4, no.1, pp. 16-30, May 2017.
- [9] C. Chen, Y. Cheng, Q. Dai, H. Song, "Radio Frequency Magnetron Sputtering Deposition of TiO<sub>2</sub> Thin Films and Their Perovskite Solar Cell Applications" *Scientific Report*, vol. 5, no. 17684, pp. 1-12, Dec. 2016.
- [10] A. Nishimura, X. Zhao, T. Hayakawa, N. Ishida, M. Hirota, E. Hu, "Impact of Overlapping Fe/TiO<sub>2</sub> Prepared by Sol-Gel and Dip-Coating Process on CO<sub>2</sub> Reduction," *Int. J. Photoenergy*, Vol. 2016, Article ID 2392581, Jun. 2016.
- [11] S. C. Ezike, A. B. Alabi, A. N. Ossai, A. O. Aina, "Effect of tertiary butylpyridine in stability of methylammonium lead iodide perovskite thin films," *Bull. Mater. Sci.*, vol. 43, issue 1, pp. 40, Jan. 2020.
- [12] S. N. Sadikin, M. Y. A. Rahman, A. A. Umar, M. M. Salleh, "Effect of Spin-Coating Cycle on the Properties of TiO<sub>2</sub> Thin Film and Performance of DSSC," *Int. J. Electrochem. Sci.*, vol. 12, pp. 5529 – 5538, May 2017.
- [13] I. Sta, M. Jlassi, M. Hajji, M.F. Boujmil, R. Jerbi, M. Kandyla, M. Kompitsas, H. Ezzaouia, "Structural and Optical Properties of TiO<sub>2</sub> Thin Films Prepared by spin Coating," *J. Sol-Gel Sci. Tech.*, vol. 72, pp. 421-427, Jul. 2014.
- [14] A. Jain, D. Vaya, "Photocatalytic Activity of TiO<sub>2</sub> Nanomaterial," *J. Chil. Chem. Soc.*, vol. 62, no.4, 2017.
- [15] V. Binas, D. Venieri, D. Kotzias, G. Kiriakidis, "Modified TiO<sub>2</sub> based photocatalysts for improved air and health quality," *Journal of Materiomics*, vol. 3, Issue 1, pp. 3-16, March 2017.
- [16] J. Spiridonova, A. Katerski, M. Danilson, M. Krichevskaya, M. Krunks, I. O. Acik, "Effect of the Titanium Isopropoxide: Acetylacetone Molar Ratio on the Photocatalytic Activity of TiO<sub>2</sub> Thin Films" *Molecules*, vol. 24, pp. 4326, Nov. 2019.
- [17] S. K. Pathak, A. Abate, T. Leijtens, D. J. Hollman, J. Teuscher, L. Pazos, P. Docampo, U. Steiner, H. J. Snaith, "Towards Long-Term Photostability of Solid-State Dye Sensitized Solar Cells" *Adv. Energy Mat.* vol. 4, 2014.
- [18] A. Fakharuddin, F. D. Giacomo, A. L. Palma, F. Matteocci, I. Ahmed, S. Razza, A. D'Epifanio, S. Licoccia, J. Ismail, A. D. Carlo, T. M. Brown, R. Jose, "Vertical TiO<sub>2</sub> Nanorods as a Medium for Stable and High-Efficiency Perovskite Solar Modules," *ACS nano*, vol. 9, issue 8, pp. 8420-8429, Aug. 2015.
- [19] K. Fischer, A. Gawel, D. Rosen, M. Krause, A. A. Latif, J. Griebel, A. Prager, A. Schulze, "Low-Temperature Synthesis of Anatase/Rutile/Brookite TiO<sub>2</sub> Nanoparticles on a Polymer Membrane for Photocatalysis," *Catalyst*, vol. 7, pp. 209, Jul. 2017.
- [20] B. N. Cardoso, E. C. Kohlrausch, M. T. Laranjo, E. V. Benvenutti, N. M. Balzaretto, L. T. Arenas, M. J. L. Santos, T. M. H. Costa, "Tuning Anatase-Rutile Phase Transition Temperature: TiO<sub>2</sub>/SiO<sub>2</sub> Nanoparticles Applied in Dye-Sensitized Solar Cells" *Int. J. Photoenergy*, vol. 2019, Article ID 7183978, Mar. 2019.
- [21] T. S. Senthil, N. Muthukumarasamy, S. Agilan, M. Thambidurai, R. Balasundaraprabhu, "Preparation and characterization of nanocrystalline TiO<sub>2</sub> thin films," *Mat. Sci. and Eng. B*, vol. 174, issue 1-3, pp. 102-104, Oct. 2010.
- [22] A. Elfanaoui, E. Elhamri, L. Boulkaddat, A. Ihlal, K. Bouabid, L. Laanab, A. Taleb, X. Portier, "Optical and structural properties of TiO<sub>2</sub> thin films prepared by sol-gel spin coating," *Int. J. Hydrogen Energy*, vol.36, issue 6, pp. 4130-4133, 2011.
- [23] V. Zharvan, R. Daniyati, A. S. N. Ichzan, G. Yudoyono, Darminto, "Effect of calcination temperature on the photocatalytic activity of TiO<sub>2</sub> powders prepared by coprecipitation of TiCl<sub>3</sub>," *Proceedings of 14<sup>th</sup> AIP international conference on theoretical and applied Physics*, vol. 1725, issue 1, pp 020099, April 2016.
- [24] S. W. Balogun, S. C. Ezike, Y. K. Sanusi, A. O. Aina "Effects of thermal annealing on optical properties of poly (3-Hexyithiophene):[6, 6]-Phenyl C60-butyric acid methyl ester blend thin film," *Journal of Photonic Materials and Technology*, vol.3, issue 2, pp. 14-19, Nov. 2017.
- [25] Weight Percent. Available <http://dl.clackamas.edu/ch105-04/weight.htm> (accessed on 27 Jan. 2020)
- [26] F. Huang, A. Yan, H. Zhao, "Influence of doping on photocatalytic properties of TiO<sub>2</sub> Photocatalyst," *Intechopen*, vol. Aug. 2016.
- [27] S.C. Ezike, D. N. Okoli, "Deposition Temperature Effects On CuAlSe<sub>2</sub> Compound Thin Films Prepared By Chemical Bath Deposition Technique" *IOSR Journal of Applied Physics*, vol. 1, issue 3, pp. 23-26, 2012.
- [28] A. K. Tripathi, M. K. Singh, M. C. Mathpal, S. K. Mishra, A. Agarwal, "Study of structural transformation in TiO<sub>2</sub> nanoparticles and its optical properties," *Journal of Alloys and Compounds*, vol. 549, pp. 114-1205, Feb. 2013.
- [29] N. Rani, S. Chahal, A. S. Chauhan, P. Kumar, R. Shukla, S. K. Singh, "X-ray Analysis of MgO Nanoparticles by Modified Scherer's Williamson-Hall and Size-Strain Method," *Materials Today: Proceedings*, vol. 12, pp. 543–548, 2019.

#### Publish your research article in AIJR journals-

- Online Submission and Tracking
- Peer-Reviewed
- Rapid decision
- Immediate Publication after acceptance
- Articles freely available online
- Retain full copyright of your article.

Submit your article at [journals.aijr.in](http://journals.aijr.in)

#### Publish your books with AIJR publisher-

- Publish with ISBN and DOI.
- Publish Thesis/Dissertation as Monograph.
- Publish Book Monograph.
- Publish Edited Volume/ Book.
- Publish Conference Proceedings
- Retain full copyright of your books.

Submit your manuscript at [books.aijr.org](http://books.aijr.org)